BIOCHEMISTRY
including biophysical chemistry & molecular biology

ARTICLE

pubs.acs.org/biochemistry

Interactions between Kinase Scaffold MP1/p14 and Its Endosomal Anchoring Protein p18†

James Magee and Miroslaw Cygler*

Biotechnology Research Institute, NRCC, 6100 Royalmount Avenue, Montreal, Quebec H4P 2R2, Canada

Supporting Information

ABSTRACT: Scaffold and adaptor proteins provide means for the spatial organization of signaling cascades. MP1 is a scaffold protein in the RAF/MEK/ERK pathway and together with p14 forms a heterodimer that was shown to be responsible for localization of MEK to the late endosomal compartment. However, the mechanism by which MP1/p14 tethers MEK to the endosomal membrane was not resolved. Recently, an adaptor protein p18 was identified as a binding partner of MP1/p14. p18 is attached to the endosomal surface by myristoyl and palmitoyl groups located at the N-terminus of the protein and tethers the signaling complex to the cytoplasmic surface of late endosomes. p18 expressed in *E. coli* is retained in inclusion bodies, and we developed a protocol to refold it from the denatured state. Coexpression of p18 with MP1/p14 leads to a soluble protein complex. We examined the interaction of p18 with the MP1/p14 constitutive heterodimer. We cloned various constructs of p18 and characterized their behavior and interactions with MP1/p14 *in vitro* using SEC and pull-down assays. We determined that the refolded p18 is a monomer in solution with molten globule characteristics. Its binding to MP1/p14 promotes folding and ordering. We also identified a proteolytically stable fragment of p18 and showed that it binds to MP1/p14 with similar affinity to the full-length construct and determined an apparent dissociation constant in the low micromolar range for the interaction. Finally, we show that the ~60 C-terminal residues of p18 are not required for *in vitro* interaction with MP1/p14 heterodimer, in contrast to previously reported findings showing that truncation of 41 C-terminal residues of p18 prevents endosomal localization of MP1/p14.

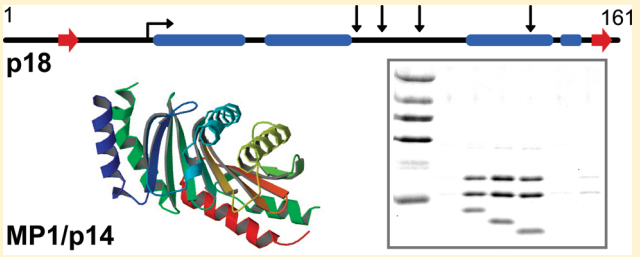

The mitogen-activated RAF/MEK/ERK protein kinase (MAPK) pathway is crucial for cellular responses to many external stimuli and transduces external signals into the cell, effecting nuclear, cytoplasmic, and cytoskeletal events. This pathway is involved in cell survival and proliferation,[1] differentiation,[2] apoptosis,[3] and other events. Disregulation of this pathway is associated with various cancers, among them cancers of the colon, pancreas, skin, thyroid, ovary, and lungs.[4] Other diseases associated with disregulation of this pathway include Noonan, LEOPARD, Costello, and cardiofaciocutaneous syndromes and neurofibromatosis type I, all of which are characterized by muscular abnormalities, mental retardation, heart defects, and distinctive facial appearance.[5]

The response of kinase pathways to external signals is moderated spatiotemporally by interactions of the kinase proteins with scaffold proteins;[6,7] among them are MP1, MEK partner 1[8] and KSR, kinase suppressor of Ras.[9] Generally, scaffold proteins enhance signal flux by bringing kinases and their substrates into close proximity in signaling complexes. Scaffolds can also activate associated kinases allosterically, further enhancing output. Furthermore, subcellular localization plays a role in signaling specificity. Various scaffolds cause activated ERK to be found in the nucleus or cytosol or associated with the cytoskeleton or with subcellular vesicles with concomitant effects on the substrates activated by ERK in each locale. Localization of the scaffold may be an intrinsic property or mediated by interaction with an adaptor protein.[6,10]

MP1, a small 14 kDa protein, was first identified as a MEK scaffold in a yeast two hybrid screen. MP1 selectively binds MEK1 and ERK1 over MEK2 and ERK2 and enhances ERK1's activation of transcription factor Elk-1.[8] Another small 14 kDa protein, p14, was shown to be part of the protein complex that localizes a branch of the MEK/ERK signaling pathway to late endosomes. MP1 and p14 interact constitutively, in contrast to MP1's dynamic association with MEK or ERK.[11] Although MEK1 binds directly to MP1 but not to p14, the latter protein is required for MEK localization to endosomes and for efficient signaling in response to EGF. While essential for endosomal targeting of MEK, p14 was shown not to be a membrane protein.[12]

MP1 forms a tight heterodimer with p14 with nanomolar affinity.[13] On its own, the heterodimer is soluble in aqueous solution. Its crystal structure showed that MP1 and p14 have very similar three-dimensional structures despite a very low level of sequence similarity.[13,14] On the other hand, both proteins individually have been highly conserved during evolution, with

Received: December 10, 2010
Revised: March 30, 2011
Published: March 31, 2011

sequence identity between human and yeast proteins of ~60%, indicating an essential cellular role.[14]

The mechanism by which the MP1/p14 scaffolding complex becomes attached to endosomes was unclear. This mechanism became apparent with the recent description of p18, a protein that interacts with the MP1/p14 complex.[15] p18 was identified in a screen of detergent-resistant membrane proteins. Detailed studies showed that p18 is required for MP1/p14 anchoring to late endosomal membranes. The first ~20 N-terminal residues of p18 are required for association with endosomes.[15] The primary sequence is predictive of a myristoyl group attached to Gly2 and palmitoyl groups attached to Cys3 and Cys4. Indeed, a large-scale study of palmitoylated proteins in mammalian cells found that p18 is both myristoylated and palmitoylated.[16] Immunoprecipitation of recombinant tagged proteins in mouse embryonic fibroblast cells as well as *in vitro* pull-down assays showed that p18 binds to both MP1 and p14 and to the MP1/p14 complex. *In vivo* studies showed that deleting 41 amino acid residues from the C-terminus of p18 abrogated this interaction. Deletion of p18 yields similar phenotypes as deletion of either p14 or MEK1, suggesting a functional link between these proteins.[15,17]

Recently, several studies have examined the role of p18. The promoter of the human p18 gene contains sterol response elements, and consequently the relationship between p18 ("Pdro" in this study) and cholesterol was examined in a human neuroblastoma cell line. A positive feedback loop between the levels of cellular free cholesterol and p18 expression was observed, with p18 expression controlled at the levels of both transcription and translation. Depletion of p18 caused an increase in trafficking of cholesterol into the cell, between subcellular compartments, and out of the cell as well as the redistribution of late endosomes/lysosomes.[18] p18 was also found in a complex including membrane-type 1 matrix metalloproteinase (MT1-MMP) in invadopodia in human melanoma cells. Despite not interacting with MT1-MMP directly, p18 (named "p27RF-Rho") was shown to play a role in these membrane protrusions required for tumor cell invasion by activating the GTPase RhoA, causing enhanced formation of actin stress fibers and enhanced invasion of synthetic basement membrane. Activation of RhoA occurs when p18 binds $p27^{kip1}$, an inhibitor of RhoA, allowing activating guanine nucleotide exchange factors to access RhoA.[19] p18, MP1, and p14 were also identified in immunoprecipitates of the GTPases RagB, RagC, and RagD prepared from human HEK293T cells. *In vitro* assays showed a direct association between the Rag proteins and p18 but no association between Rag and MP1 or p14. The MP1/p14/p18 complex (collectively termed "Ragulator") is necessary for association of the Rag proteins with the late endosomal/lysosomal surface. Upon stimulation of the cells by amino acids, Rag becomes GTP-loaded and recruits the mTORC1 kinase to the membrane where it can be activated by Rheb.[20] There may be a connection between the mTORC1 and MEK/ERK signaling pathways via PI3K, Akt, and Raf, in addition to a direct relationship via p18/MP1/p14.

Here we describe cloning, expression, and purification of the p18 protein and the investigation of its interactions with the MP1/p14 complex *in vitro*. p18 expressed on its own is retained in inclusion bodies but can be refolded, while when coexpressed with MP1/p14 it forms soluble complex. We show that p18 undergoes binding-induced ordering and folding as it interacts with MP1/p14. We have further examined the segment of p18 required for interaction with MP1/p14 and determined an apparent dissociation constant for the binding of p18 to MP1/p14.

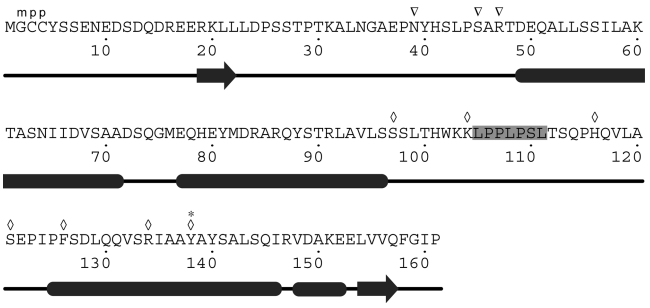

Figure 1. Primary sequence of mouse p18. The predicted secondary sequence, as determined by PSIPRED,[21] is indicated by arrows for β-strands and thick lines for α-helices; predicted myristoylation (m) and palmitoylation (p) sites are indicated above the sequence.[15] Various p18 constructs were expressed with N-termini (∇) and C-termini ($\Diamond$) as indicated, including that corresponding to a proteolytically truncated form (*) of p18. A deleted proline-rich predicted loop region from residues 105−111 is highlighted.

MATERIALS AND METHODS

Cloning and Expression of p18. Mouse cDNA encoding p18 was obtained from the PlasmID DNA resource (Harvard University, Cambridge, Massachusetts). Sequence analysis indicated that the first ~45 residues are disordered and that the remainder of the protein is highly α-helical (InterProScan, DISOPRED[21] and PSIPRED[22] servers, see Figure 1). We subcloned residues 39−161, 45−161, and 47−161 into vectors pJW234 (a derivative of pET15b vector, His-TEV N-terminal tag) and pRL652 (a derivative of pGEX-4T1 vector, GST-TEV N-terminal tag) using *Bam*HI and *Eco*RI restriction enzyme sites for both vectors. As an example, for the 47−161 construct the forward oligonucleotide was 5′-AAA**GGATCC**CGCACAGATGAGCAGGC-3′ and the reverse oligonucleotide was 5′-AAA**GAATTC**TCATGGTATCCCAAACTGTACAACC-3′, with restriction sites indicated in bold. The expression of these six p18 constructs was tested in BL21(DE3) and Rosetta.pLysS strains of *E. coli*, and in both strains the protein was found in inclusion bodies. In order to improve the yield of soluble p18, we tried to express the GST-p18 construct in the presence of chaperones (dnaK, dnaJ, grpE, groES, and groEL) expressed from the pG-KJE8 plasmid (TakaraBio, Madison, WI). No improvement in solubility of p18 was found. We also tried to coexpress p18 with MP1/p14 inserted into the two cloning sites of the pCDF-Duet vector (for construct details, see ref 14). Expression of MP1/p14 was very low, and p18 was not found in the soluble fraction when expression was tested in BL21(DE3) cells.

Purification and Refolding of p18. Rosetta.pLysS cells expressing His-tagged p18(47−161) were lysed by sonication in PBS, and insoluble material was resuspended in the same buffer containing 8 M urea. IMAC was performed using buffers containing 8 M urea and p18 was eluted under denaturing conditions. Refolding of p18 was tested in 96 conditions by a 1:10 dilution into the final condition.[23] 100 mM glycine buffer, pH 9.0, 200 mM NaCl was identified as the best condition for p18 refolding. Large-scale refolding was by dilution into a large volume of buffer (50 mM Tris pH 8.9, 0.2 M NaCl, 0.4 M arginine, 0.1 M urea, 1 mM DTT), with and without MP1/p14 present. In both cases, p18 was at 0.01 mg/mL. MP1/p14 was present in equal molar ratio. Refolding continued for 1, 3, or 5 days prior to concentrating p18 or p18/MP1/p14 in an Amicon

stirred-cell concentrator with a 3 kDa membrane. Refolding of p18 and binding to MP1/p14 were analyzed by SEC.

Characterization of Proteolytic Fragment of p18. During refolding we observed by SDS-PAGE partial proteolysis of p18. The refolded and purified p18 was analyzed by Western blot with anti-His antibody to confirm the presence of the amino-terminal His-tag. The expected MW of the expressed protein is 15 783 Da; however, mass spectrometry showed a molecular weight of 13 267 Da, indicating a C-terminal truncation after residue 138 (Figure 1). A new construct corresponding to the purified truncated protein was produced by replacing codon 139 with a stop codon using standard site-directed mutagenesis protocols. The new construct, His-p18(47−138), was purified and refolded in the same manner as above.

Creation of Internal Loop Deletion Mutant. An internal deletion of predicted loop residues 105−111 (Figure 1) was created using the SLIM technique.[24] Expression of this new construct, His-p18(47−138Δ105−111), was tested in the BL21(DE3) and BL21-AI (Invitrogen, Burlington, Ontario) strains of *E. coli*, with and without coexpression of MP1/p14 (also His-tagged). Expression in the BL21-AI strain led to an increase in MP1/p14 expression, and in this case we found p18 in the soluble fraction in complex with MP1/p14. Prior to lysis, cells were treated with lysozyme/EDTA to remove the outer membrane/periplasm.[25] Complexes were purified by IMAC followed by SEC to separate p18/MP1/p14 complexes from MP1/p14 complexes.

Characterization of p18 Amino Acids Required To Interact with MP1/p14. GST-p18(47−161) was mutated to produce various carboxy termini: S97, K104, H116, S121, F126, R134, and Y138 (Figure 1). Interaction was determined by pull-down of p18 from the soluble fraction of BL21-AI *E. coli* lysates from cells coexpressing His-tagged MP1/p14 and GST-p18 using IMAC resin. Material eluted from IMAC resin was bound to glutathione sepharose and proteins were eluted by TEV cleavage of the GST tag from p18. Eluted complexes were analyzed by SDS-PAGE.

Circular Dichroism Spectroscopy. Protein buffer was exchanged for 10 mM Tris-sulfate, pH 8.8, 20 mM NaF using SEC. CD spectra were measured using a 1 mm path-length cuvette in a Jasco J-815 CD spectrometer. All spectra were corrected for the signal arising from buffer alone.

Fluorescence Titration of p18 with MP1/p14. The intrinsic tryptophan fluorescence of p18 was measured with a Varian Cary Eclipse fluorescence spectrophotometer while being titrated with MP1/p14. His-p18(47−138) was purified and refolded as above, and p18 was purified by SEC using a Superdex 75 10/300 column. His-MP1/His-p14 was purified by IMAC followed by SEC on the same column. The final buffer in both cases was 10 mM Tris, pH 8.8, 150 mM NaCl, 5% (v/v) glycerol. 10 μM p18 was titrated at room temperature with MP1/p14 from 0 to 30 μM final concentration. Tryptophan residues were specifically excited at a wavelength of 295 nm, and the fluorescence emission was measured and integrated between 310 and 410 nm. The average of five scans was used for each measurement. The same titration was performed in the absence of p18 (MP1/p14 titrated into buffer) and in the absence of MP1/p14 (dilution of p18). All measurements were corrected for the fluorescence signal due to buffer alone. Complex formation was measured as the difference between the fluorescence of p18 in the presence of MP1/p14 and the sum of the individual fluorescence measurements of p18 and MP1/p14. The differential fluorescence ΔF is proportional to

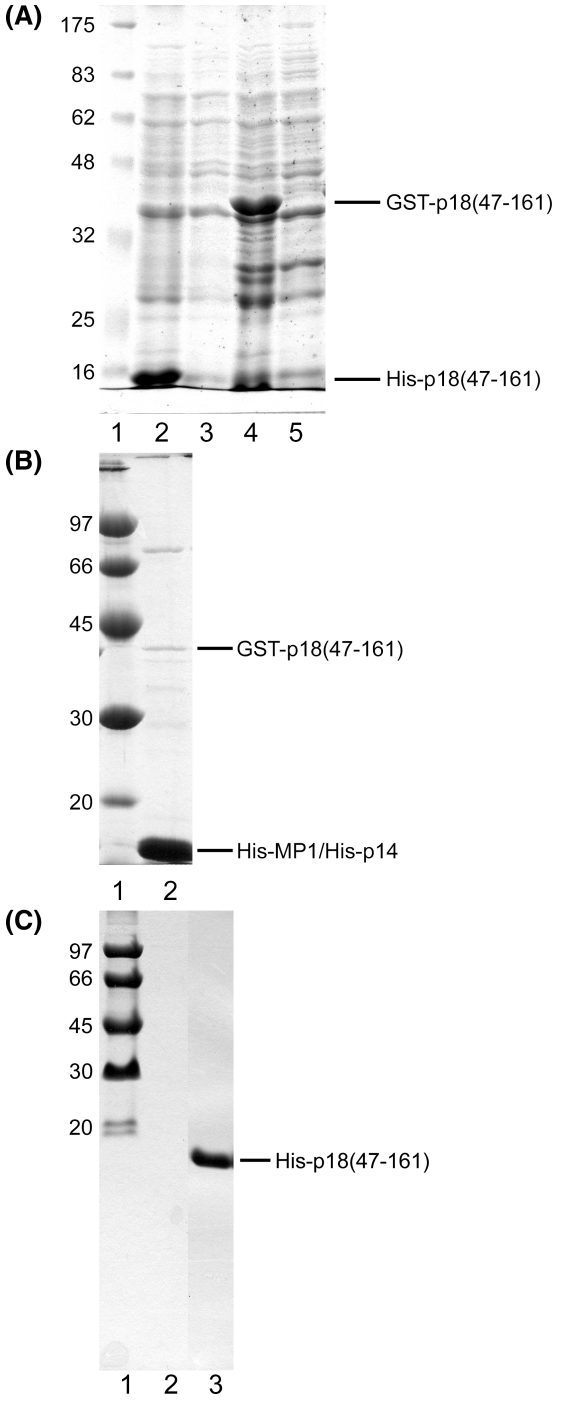

Figure 2. Expression and purification of p18. (a) Small-scale expression of initial p18 constructs in Rosetta.pLysS strain. Lane 1, molecular mass standards (kDa). His-p18(47−161), predicted molecular mass 15.9 kDa; lane 2, total lysate; lane 3, soluble fraction GST-p18(47−161), predicted molecular mass 39.4 kDa; lane 4, total lysate; lane 5, soluble fraction. (b) Pull-down of p18 by MP1/p14. Lysates containing poorly soluble GST-p18(47−161), predicted molecular mass 39.4 kDa, and His-MP1/His-p14 were mixed together. Proteins purified by IMAC were analyzed by SDS-PAGE. Lane 1, molecular mass standards (kDa); lane 2, IMAC elution fraction. (c) IMAC purification under denaturing conditions of His-p18(47−161), predicted molecular mass 15.9 kDa. Lane 1, molecular mass standards (kDa); lane 2, on-column refolding followed by elution with 250 mM imidazole under native conditions. Precipitated protein remained on the column. Lane 3, precipitated protein could be eluted after addition of 8 M urea.

the concentration of the complex

$$\Delta F = F(\text{p18/MP1/p14}) - F(\text{p18}) - F(\text{MP1/p14}) = y[\text{p18/MP1/p14}] \quad (1)$$

where y is a constant dependent on the particulars of the fluorophore and fluorescence spectrophotometer. The K_d for the association of p18 with MP1/p14 has the following form, where subscript "0" indicates the total concentration of a species:

$$\begin{aligned} K_d &= [\text{p18}][\text{MP1/p14}]/[\text{p18/MP1/p14}] \\ &= \{[\text{p18}]_0 - [\text{p18/MP1/p14})]\}\{[(\text{MP1/p14})]_0 \\ &\quad - [\text{p18/MP1/p14}]\}/[\text{p18/MP1/p14}] \\ &= \{[\text{p18}]_0 - \Delta F/y\}\{[\text{MP1/p14}]_0 - \Delta F/y\}/(\Delta F/y) \quad (2) \end{aligned}$$

Data were fit to this equation using a least-squares method to solve for K_d and y and taking into account the dilution of each protein as MP1/p14 was titrated into the cuvette.

Isothermal Titration Calorimetry of p18 Interaction with MP1/p14. His-p18(47−138) and His-MP1/His-p14 were purified as for fluorescence titration, and their interaction was measured using a MicroCal ITC200 microcalorimeter. The cell contained 200 μL of p18 at 51.0 μM while the syringe contained 287 μM MP1/p14. After an initial injection of 1 μL, 2 μL injections were performed until a total of 39 μL of MP1/p14 had been injected into the cell. The cell was stirred at 1000 rpm during the entire experiment. Data were analyzed using the included Origin software with the "One Site" model (assuming n equivalent binding sites for the ligand on its acceptor molecule) and specifying that the ligand was found in the calorimeter cell.

RESULTS

Analysis of p18 Amino Acid Sequence. The mouse and human p18 genes code for proteins of 161 amino acid residues. Their primary sequences were analyzed for the presence of secondary structures and potential for intrinsically disordered regions. There are strong predictions of three α-helical regions (~50−70, ~78−95, ~125−145) and one short β-strand (154−157), with the exact boundaries varying somewhat between the programs. A second β-strand (117−120) was predicted with lower probability (Figure 1). The N-terminal ~45 residues lack secondary structure and were predicted by several programs to be intrinsically disordered. On the basis of these, we designed N-terminally truncated constructs of p18, 39−161, 45−161, and 47−161, with the majority of the disordered region being deleted.

Recombinant p18(47−161) Binds MP1/p14 Heterodimer. The three His-tagged p18 constructs expressed well in Rosetta. pLysS cells but were insoluble. We continued with the shortest construct that had the entire predicted disordered region removed. When expressed with the GST tag, a small fraction of expressed protein was soluble (Figure 2a). To further improve its solubility, we coexpressed it with (1) a plasmid containing several chaperones or (2) a compatible pCDF-Duet plasmid carrying MP1/p14. However, in both cases most p18 protein was still found in inclusion bodies.

Since expression of GST-p18 led to small amounts of soluble protein, we tested by pull-down if this protein binds the MP1/p14 complex. Lysates of cells individually expressing GST-p18(47−161) and His-MP1/His-p14 were mixed together, and the resulting mixture was purified by IMAC. Proteins were eluted with imidazole and analyzed by SDS-PAGE. All three

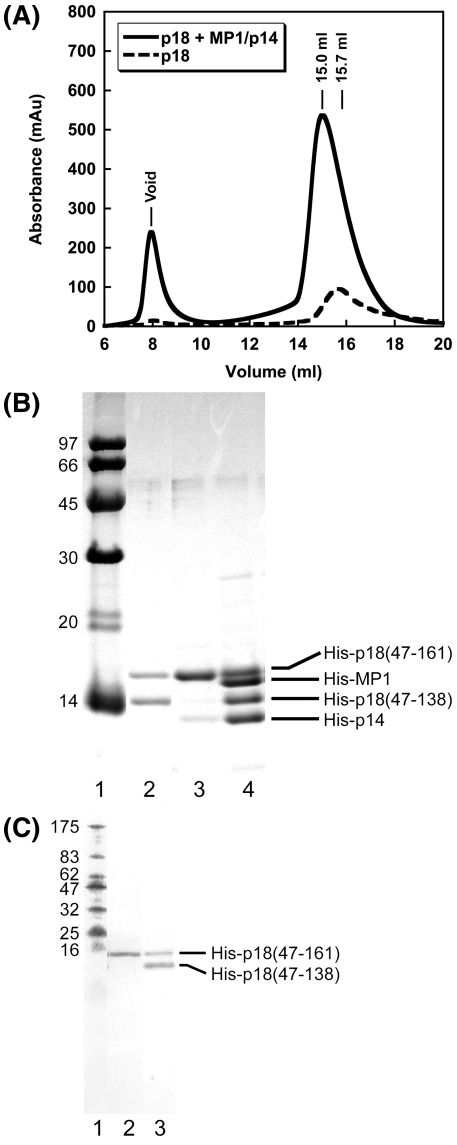

Figure 3. Size exclusion chromatography of p18 and p18+MP1/p14 complex. (a) His-p18(47−161) refolded in the absence (dotted line) and presence (solid line) of His-MP1/His-p14, analyzed on a Superdex 200 10/300 GL column. (b) SDS-PAGE of fractions from (a) lane 1, molecular standards; lane 2, peak fractions for p18 alone (dashed line, 15.7 mL); lane 3, void peak for p18+MP1/p14 (solid line); lane 4, peak for p18+MP1/p14 (solid line, 15.0 mL). (c) Anti-His-tag Western blot of samples from (b); lane 1, molecular mass standards (kDa); lane 2, void peak containing only uncleaved protein; lane 3, the main peak fraction of p18 with uncleaved and cleaved protein.

proteins were present indicating formation of a p18/MP1/p14 complex (Figure 2b). The small amount of GST-p18 eluted precluded further analysis of the complex.

Refolding of p18. The p18(47−161) construct retained binding to MP1/p14, and considering this is a small protein without cysteines, we purified denatured His-p18(47−161) and determined conditions for its refolding. Attempts to refold this denatured p18 protein construct bound to an IMAC column by washing with a decreasing gradient of urea in PBS were unsuccessful. Therefore, bound p18 was eluted with imidazole under denaturing conditions, and this highly pure denatured protein (Figure 2c) was screened for refolding using 96 different

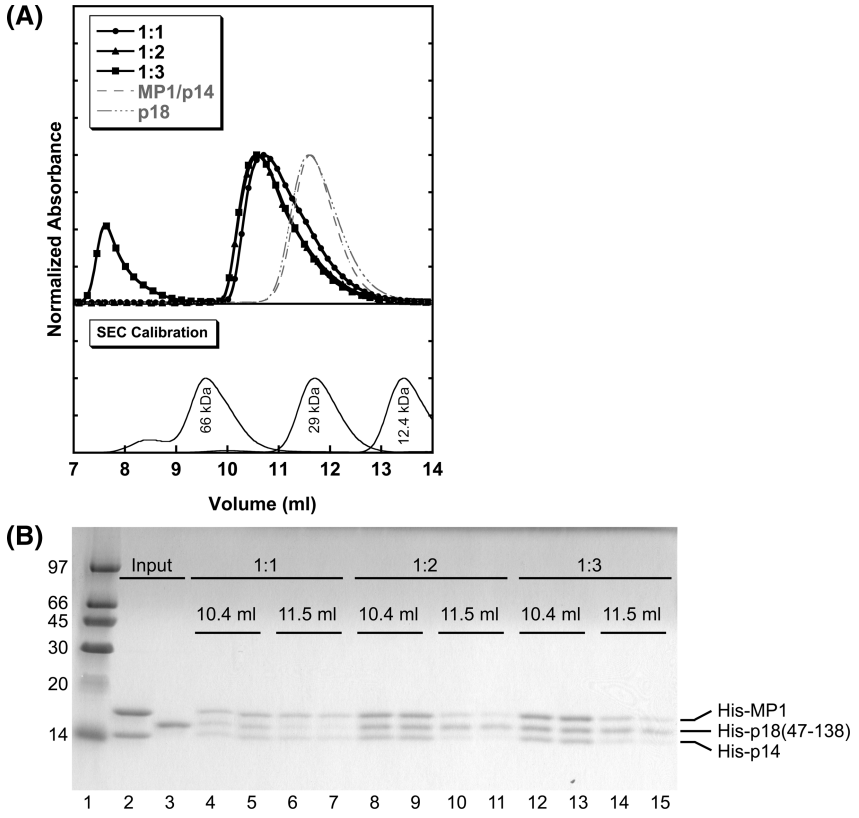

Figure 4. Stoichiometry of MP1/p14 and p18 interaction. His-MP1/His-p14 was mixed with refolded His-p18(47−138) in stoichiometric ratios of 1:1, 1:2, and 1:3 MP1/p14:p18; the mixtures and input proteins were analyzed by SEC on a Superdex 75 10/300 GL column. (a) Top panel: SEC elution profiles of mixtures and input proteins (traces for 1:2 and 1:3 overlap between 10 and 13 mL); bottom panel: column calibration was performed by individual injection of protein mass standards bovine serum albumin (66 kDa monomer), carbonic anhydrase (29 kDa), and cytochrome *c* (12.4 kDa). (b) SDS-PAGE of elution fractions from (a). Lane 1, molecular mass standards (kDa); lanes 2−3, input proteins MP1/p14 and p18; lanes 4−15, two fractions centered at 10.4 mL and two fractions centered at 11.5 mL for each ratio of MP1/p14:p18.

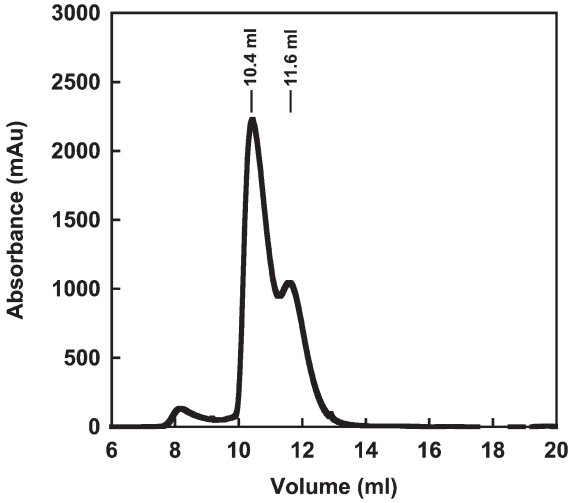

Figure 5. SEC of His-p18(47−138Δ105−111)/MP1/p14 complex. His-p18(47−138Δ105−111) was coexpressed with MP1/p14, purified by IMAC, and analyzed by SEC on a Superdex 75 10/300 GL column. The main peak is the ternary complex while the shoulder contains excess MP1/p14, as determined by SDS-PAGE.

conditions containing a variety of buffers.[23] Successful refolding was determined by a lack of optical density at 340 nm that is characteristic of precipitated protein. We identified high pH and 200 mM NaCl as the main factors affecting refolding and selected Tris buffer for large-scale refolding experiments augmented with 400 mM arginine and 100 mM urea as these are common additives used for protein refolding.[23] The yield of refolded p18 was evaluated after 1 day (overnight), 3 days, and 5 days. Five days at a protein concentration of 10 μg/mL gave the best yield of refolding amounting to ∼15% of the initial amount of protein recovered after concentration. The elution profile of His-p18(47−161) analyzed on a Superdex 200 column indicated an apparent molecular weight of ∼40 kDa (Figure 3a). The calculated mass of His-p18(47−161) is 15.9 kDa. We further characterized this refolded protein by dynamic light scattering. The measurements showed that after concentrating the peak fraction to 1.7 mg/mL, p18 was present as a highly polydisperse solution of large aggregates.

Refolding of p18 in the Presence of MP1/p14 Heterodimer. Since full-length p18 interacts with MP1/p14 heterodimer[15] and MP1/p14 was able to pull down p18(47−161), we reasoned that the presence of MP1/p14 during refolding may improve the yield of p18. Indeed, the presence of stoichiometric amounts of MP1/p14 during refolding of His-p18(47−161) led to recovery of essentially 100% of p18 after 5 days. Reducing agent was added to the refolding solution as both MP1 and p14 have free sulfhydryl groups. The constitutive MP1/p14 heterodimer has a mass of 30.1 kDa. Most of the protein concentrated from the refolding mixture eluted from SEC as a single peak with apparent molecular weight of ∼48 kDa,

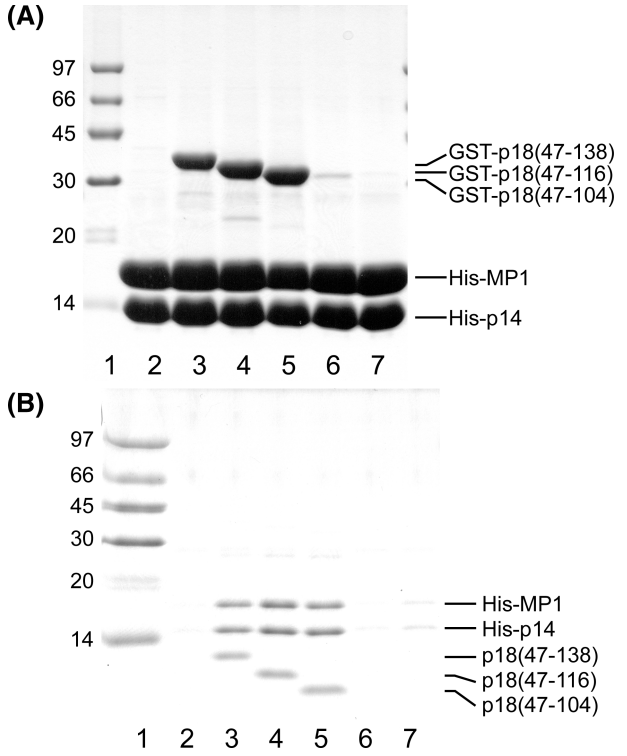

Figure 6. Interaction of MP1/p14 with truncated p18 constructs using both His-tag and GST as affinity tags. (a) IMAC elution fractions of His-MP1/His-p14 coexpressed with various TEV-cleavable GST-p18 constructs. Lane 1, molecular mass standards (kDa); lane 2, p18(47−161); lane 3, p18(47−138); lane 4, p18(47−116); lane 5, p18(47−104); lane 6, p18(47−97) (this construct expressed poorly); lane 7, control with empty vector expressing only GST. (b) p18/MP1/p14 complexes eluted in (a) were applied to glutathione sepharose and eluted with TEV; lanes labeled as in (a).

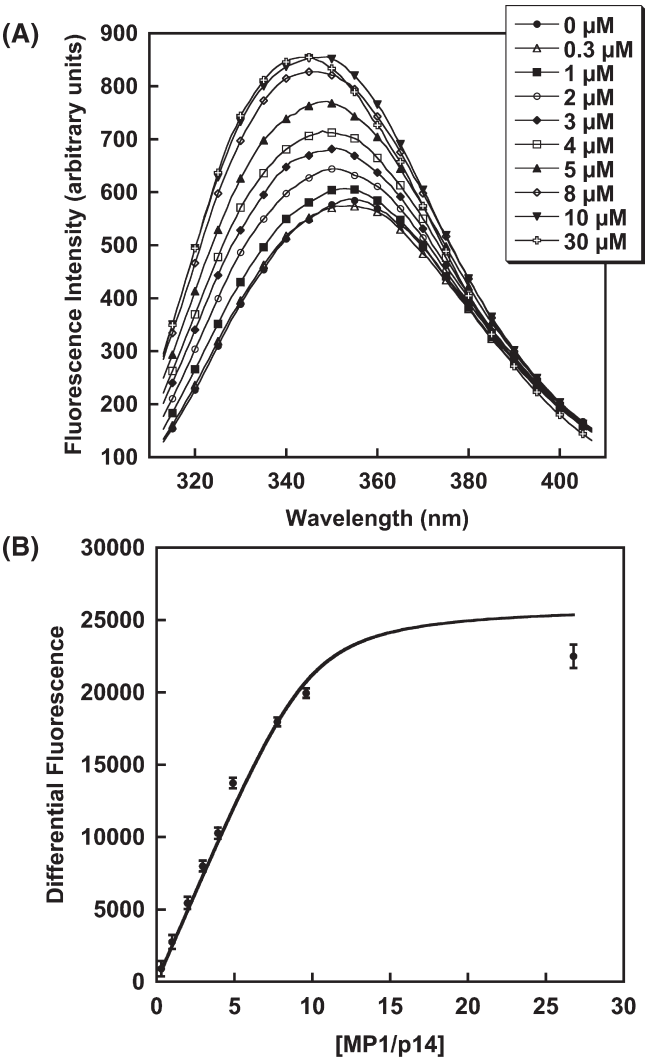

Figure 7. Fluorescence titration of p18 with MP1/p14. (a) Intrinsic tryptophan emission spectra of 5 μM p18 homodimer titrated with 0 to 30 μM MP1/p14 heterodimer. Spectra have been corrected for MP1/p14 fluorescence and smoothed. (b) Integrated fluorescence emission was used to calculate the differential fluorescence of p18 titrated with MP1/p14, which was fit to eq 2 to determine the value of K_d.

while some eluted in the void volume, indicating the presence of aggregates (Figure 3a). The protein that eluted in the void volume contained only p18. The SDS-PAGE gel of the peak fractions from SEC elution showed the presence of all three proteins (Figure 3b). DLS analysis of the peak fraction showed a solution containing large aggregates along with a species with an estimated molecular weight of 53 kDa and 20% polydispersity, in good agreement with SEC.

C-Terminal Truncation of p18 Protein. After refolding of His-p18(47−161) with or without MP1/p14 we observed the appearance of a lower molecular weight species by SDS-PAGE (Figure 3b). This species produced a signal upon Western blotting with an anti-His-tag antibody, suggesting that this is a proteolytically C-terminally truncated p18 (Figure 3c). Mass spectrometry of peak elution fractions of p18 indicated the presence of two major species with molecular weights of 15 783 and 13 267 Da (Supporting Information Figure 1). The first species corresponds to the expected p18 construct minus the initial methionine residue (calculated MW = 15 782 Da). The second species is 2516 Da smaller, which corresponds to a loss of 23 amino acids from the C-terminus to Y138 (calculated MW = 13 267 Da).

This p18(47−138) fragment was found in SEC elution peaks together with p18(47−161) and p18(47−161)/MP1/p14 but not in the void volume peak (Figure 3a,b). We concluded that this fragment is more stable than the parent protein and retains the ability to bind MP1/p14. We therefore decided to make the construct corresponding to this fragment by site-directed mutagenesis. This His-p18(47−138) refolded on its own with better yield than His-p18(47−161) (~30% and ~15%, respectively) and in the presence of MP1/p14 leads also to full recovery. This construct (calculated molecular mass of 13.4 kDa) eluted from the Superdex-75 column with apparent molecular mass of ~30 kDa, at nearly the same volume as the MP1/p14 heterodimer (Figure 4a).

To assess the folding state of the refolded, soluble p18 we measured the circular dichroism spectrum of His-p18(47−138) (Supporting Information Figure 2). The analysis of the spectrum gives ~10% of helical structure vs 40% predicted from the sequence. In addition, comparison of the $[\theta]_{200}$ and $[\theta]_{222}$ of the CD spectrum of p18 shows that it attains a premolten globule state.[26] We conclude that p18 on its own is only partially folded under these conditions and attains a premolten globule state. The apparent molecular mass for such a more loosely packed structure measured by methods such as size exclusion chromatography is usually ~3 times its real molecular mass.[26] When this p18 construct

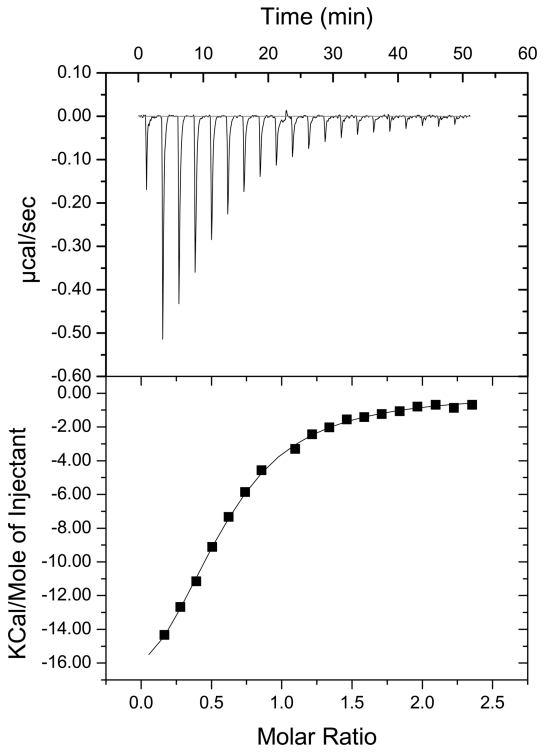

Figure 8. ITC of His-p18(47−138) titrated with MP1/p14 complex. The cell contained 200 μL of p18 at 51.0 μM while the syringe contained 287 μM MP1/p14. After an initial injection of 1 μL, 2 μL injections were performed until a total of 39 μL MP1/p14 had been injected into the cell. (a) Time course of heat evolved during ITC experiment. (b) Data were analyzed using the included Origin software with the "One Site" model (assuming *n* equivalent binding sites for the ligand on its acceptor molecule) and specifying that the ligand was found in the calorimeter cell.

was denatured in 8 M urea and subjected to size exclusion chromatography, its apparent molecular mass increased, as expected,[26] to even larger value of ∼90 kDa (Supporting Information Figure 3).

To verify if this shorter His-p18(47−138) construct binds MP1/p14, we mixed the proteins and loaded them on Superdex-75 SEC. The position of the main peak shifted to lower volume, and SDS-PAGE of the peak fractions showed the presence of all three proteins, indicating retention of binding (Figure 4). We next analyzed the CD spectra of the p18/MP1/p14 complex and derived the p18 spectrum by subtracting the spectrum of MP1/p14 alone. The difference spectrum shows ∼32% of helical structure vs predicted ∼40%. We conclude that p18 undergoes substantial ordering upon binding to MP1/p14. This p18/MP1/p14 complex eluted from the Superdex-75 column at a volume corresponding to the apparent molecular mass of 45 kDa (Figure 4) which would correspond to a 1:1:1 stoichiometry.

In order to verify the stoichiometry of p18 and MP1/p14 in the complex, we mixed them in ratios of 1:1:1, 2:1:1, and 3:1:1 and performed SEC. In all cases the maximum shifted to ∼45−50 kDa and the peak was highly asymmetric with a trailing shoulder, indicating the presence of unbound proteins. When mixed in a 1:1:1 ratio, the shoulder contained MP1/p14 but also p18, with a 2:1:1 ratio the shoulder contains a small excess of p18, while in a 3:1:1 ratio we observed also an aggregated p18 in the void volume (Figure 4). These experiments, together with the position of the p18/MP1/p14 peak at 45 kDa, suggest the stoichiometry of 1:1:1.

Loop Deletion Mutant. The inspection of the amino acid sequence of p18 showed the presence of a proline-rich segment in region 106−125 with three of them in a hydrophobic stretch of amino acids 105−111 (Figure 1). We decided to test if this stretch contributes to the aggregating properties of p18 and if it is involved in binding to MP1/p14. We created a new construct, His-p18(47−138Δ105−111), and expressed it in Rosetta.pLysS *E. coli* as well as in another strain, BL21-AI, that expresses the T7 RNA polymerase under control of an arabinose-inducible promoter. No significant improvement in protein solubility was observed as this protein was also retained in inclusion bodies. However, we noticed that BL21-AI showed significantly higher expression level than the Rosetta.pLysS strain. Therefore, we selected the BL21-AI strain for coexpression of His-p18-(47−138Δ105−111) with His-MP1/His-p14 in the pCDF-Duet vector. The expression level of all three proteins was very high (∼120 mg/L), and all three proteins were present in the soluble fraction. Gel filtration of metal affinity purified proteins showed two peaks, one containing p18(47−138Δ105−111)/MP1/p14 and the second containing excess MP1/p14 (Figure 5), as determined by SDS-PAGE.

Coexpression of His-p18(47−138) with MP1/p14 in BL21-AI strain yielded similar results. Since no significant difference between the behavior of His-p18(47−138) and Hisp18(47−138Δ105−111) was found, we did not investigate the loop-deletion mutant any further.

Other C-Terminal Truncations. Experiments *in vivo* showed that deletion of the C-terminal 41 residues (p18Δ120) is sufficient to disrupt localization of MP1/p14 to the endosomal membrane.[15] In order to better define the region of p18 necessary for binding to MP1/p14, we made additional truncations of the C-terminus of p18 and investigated their binding to MP1/p14 *in vitro*. The truncated constructs contained N-terminal, TEV-cleavable GST tag with residue 47 as the N-terminus and residues 97, 104, 116, 121, 126, 134, or 138 as the C-termini (Figure 1). These constructs were coexpressed with His-MP1/His-p14 in BL21-AI cells.

Soluble proteins were purified first by metal affinity and then glutathione affinity chromatography. In the second step, p18-containing complexes were eluted by cleaving the GST tag from p18 with TEV protease while proteins were bound to the glutathione sepharose column. SDS-PAGE of fractions eluted from both chromatography steps indicate that p18 can be truncated to Lys104 at the C-terminus and still retained binding to MP1/p14 (Figure 6). Surprisingly, the expression level of His-p18(47−161) was very low (Figure 6, lane 2), and the construct ending at amino acid Ser97 was also poorly expressed, which suggest that a weak band corresponding to the latter (Figure 6, lane 6) is either due to low amount of this construct or weaker binding to MP1/p14.

Determination of Dissociation Constant of p18 Binding to MP1/p14. The intrinsic fluorescence of the single tryptophan in p18, Trp102, was measured as p18 was titrated with MP1/p14. MP1 has no tryptophan residues while p14 has a single tryptophan, Trp53, but its fluorescence is quenched by nearby charged residues (PDB: 1SKO),[14] and its fluorescence emission intensity is less than 30% of an equimolar amount of p18; fluorescence titration measurements were corrected for this signal using a blank titration lacking p18.

The titration of p18(47−138) with MP1/p14 caused both an increase in the intrinsic tryptophan fluorescence of p18 and a decrease in the wavelength of maximum emission intensity

(Figure 7a). Refolded p18(47−138) in solution has a λ_{em}(max) of ∼354 nm, consistent with a tryptophan residue fully exposed to aqueous solution.[27] As p18 is titrated with MP1/p14, the fluorescence emission blue-shifts to 337 nm and increases in intensity. This is consistent with the p18 Trp102 moving from a polar, aqueous environment to a less polar environment as a result of MP1/p14 binding.

The differential fluorescence of p18 in the presence of MP1/p14 is proportional to the amount of complex in solution and can be used to determine the binding constant of the interaction. Because the emission wavelength maximum shifts over the titration, integrated total fluorescence was used to monitor complex formation instead of fluorescence intensity at a single wavelength.[27] Using a stoichiometry of 1:1:1 for the p18/MP1/p14 complex, we calculated the $K_d = 0.50 \pm 0.18\ \mu$M (Figure 7b).

We also examined the interaction of p18 with MP1/p14 using isothermal titration calorimetry. We performed these experiments with the most stable His-p18(47−138) construct. Since p18 is prone to aggregation at higher concentration, it was placed in the calorimeter cell at a concentration of 51 μM and titrated with MP1/p14 at 287 μM. Binding was exothermic, and data were measured until the heat evolved reached a minimum (Figure 8). Using a model of n equivalent sites for p18 on the MP1/p14 molecule yields a stoichiometry of 3.55 p18 molecules binding MP1/p14 with a $K_d = 18.2 \pm 1.2\ \mu$M. The interpretation of these data is complicated by two factors: (1) since the p18 in the cell could be partially aggregated and the aggregates unfit for binding MP1/p14, the "effective" concentration of p18 might be lower than used in these calculations, overestimating n and underestimating K_d; and (2) the binding event involves also some level of ordering of p18 which effect on the thermodynamics is difficult to quantify. Therefore, from this experiment we only conclude that the K_d has a low μM value.

DISCUSSION

The protein p18 has been identified as an endosomal anchor for the MEK/ERK scaffold MP1/p14 heterodimer. It was also shown that p18 interacts with several other proteins including $p27^{kip1}$ and Rag GTPases. *In vivo* studies showed that a deletion of the C-terminal 41 residues resulted in mislocalization of MP1/p14, indicating that the C-terminus of p18 is important for the retention of MP1/p14 heterodimer at the endosome and implicating this region as participating in interaction with the heterodimer.[15] We wanted to examine in more detail the binding of p18 to MP1/p14 and to define the region of p18 that is involved in this interaction.

We have previously expressed the MP1/p14 heterodimer and determined its crystal structure.[14] We therefore attempted to express recombinant p18 in *E. coli*. p18 has no recognizable similarity to any protein with known three-dimensional structure, and we performed bioinformatic analysis to identify the location of secondary structure elements and assess the propensity for intrinsically disordered regions. In addition to predicted myristoylation and palmitoylation sites, the N-terminal portion of the protein (∼45 residues) showed features typical for intrinsically unfolded regions,[21] and we used this information to exclude most of this region in the design of our constructs. Despite the small size of the protein and the lack of cysteines in the constructs, the expressed protein variants were almost completely insoluble. However, we were able to develop a refolding protocol that resulted in recovery of soluble p18 variants. In addition, the refolding yield was significantly augmented by the presence of MP1/p14. Circular dichroism spectra indicate that the refolded p18 protein appears to be only partially folded, in a premolten globule state, with only ∼10% of helical structure rather than 40% predicted from the sequence. The association of p18 with MP1/p14 promotes its folding. With this result, we attempted to coexpress p18 together with MP1/p14 and were able to obtain soluble complex containing all three proteins. The stoichiometry of p18/MP1/p14 complex appears to be 1:1:1.

A series of C-terminal truncations allowed us to narrow down the region of p18 involved in binding the MP1/p14 scaffold to residues ∼47−104. This region is predicted to form two hairpin α-helices connected by a short loop and excludes the predicted long C-terminal α-helix (Figure 1). However, *in vivo* experiments indicated that a segment beyond residue 120 is necessary for localization of the MP1/p14 scaffold to the endosomes as a p18(1−120) construct failed to correctly localize the scaffold,[15] leading the authors to conclude that p18(1−120) does not bind MP1/p14. Recent reports that p18 interacts with several other proteins suggest a possible explanation for this discrepancy.[19,20] p18 is involved in large signaling complexes, and we hypothesize that proper localization of MP1/p14 may require contacts with other partners in addition to p18. The C-terminal ∼40 residues of p18 (predicted to form a long α-helix) may be essential for these other interactions while it is not necessary for the formation of a p18/MP1/p14 complex *in vitro*.

We have previously tried to isolate *in vitro* the MEK1 kinase bound to the MP1/p14 scaffold (MP1/p14/MEK1 ternary complex). Our results suggest that MP1 on its own may not be able to simultaneously bind p14 and MEK1 (unpublished data). In addition, while MP1/p14 forms a very tight heterodimer, it is the p18/MP1/p14 complex ("Ragulator") that is the functional unit for kinase scaffolding on the surface of late endosomes/lysosomes.[20] We therefore hypothesize further that p18 is required for the simultaneous interaction of MP1 with MEK1 and p14 observed *in vivo*.[12]

Using two different methods, we obtained the apparent dissociation constant of the p18 homodimer with MP1/p14, which while they differ, they both indicate low micromolar range. This is a much weaker interaction than the nanomolar affinity of MP1 and p14. This weak interaction between subunits of a functional complex again suggests that other proteins may be required to form a robust signaling complex. It may further indicate that p18 and MP1/p14, while active together in the Ragulator complex, also have individual functions that require dissociation.

There is growing evidence for involvement of the Ragulator complex in cell motility, cell spreading, and tumor invasion. This complex serves as a scaffold in several kinase pathways, such as MEK/ERK and mTORC1 (via Rag), and p18 controls Rho by binding its inhibitor, $p27^{kip1}$. p18 shares some interesting similarities with $p27^{kip1}$.[19] $p27^{kip1}$ binds the CDK2/cyclin A complex, and its N-terminal segment has been crystallized in this trimeric complex.[28] $p27^{kip1}$ has been shown to interact individually with both CDK2 and cyclin A *in vitro*, and the crystal structure shows that this is because $p27^{kip1}$ binds to the surface of the kinase/cyclin complex in an extended conformation that wraps around both binding partners.[28,29] Likewise, p18 is capable of binding both MP1 and p14 individually as well as the heterodimer.[15] In addition, $p27^{kip1}$ lacks a rigid structure in its unbound form, although there is some residual secondary structure as determined by CD and NMR. $p27^{kip1}$ binds to the CDK2/cyclin A complex by first binding

cyclin A, then undergoing a folding reaction, and then finally associating with CDK2, which also undergoes a binding-induced conformational change upon association with $p27^{kip1}$.[29] Similarly, p18 is a premolten globule in solution; it becomes ordered and folded as it binds to MP1/p14. While there is little to no sequence similarity between p18 and $p27^{kip1}$, both proteins are relatively small molecules with many binding partners that are involved in networks of kinase signaling pathways. Thus, it seems reasonable to assume that p18, like $p27^{kip1}$, uses structural flexibility as a means to accommodate numerous interactions in a small protein. Our data support the role of additional proteins in the formation of competent signaling complexes on late endosomes.

■ ASSOCIATED CONTENT

Supporting Information. Mass spectrometry spectrum of the refolded p18; CD spectra of p18, MP1/p14, and p18/MP1/p14; and SEC profile of refolded p18 and p18 solubilized in urea. This material is available free of charge via the Internet at http://pubs.acs.org.

■ AUTHOR INFORMATION

Corresponding Author

*Tel: 514-496-6321. Fax: 514-496-5143. E-mail: mirek@bri.nrc.ca.

Notes

[†]This is NRCC Publication No. 53140.

■ ACKNOWLEDGMENT

We thank Dr. R. Menard for help with the analysis of fluorescence data, Dr. G. Kozlov for help with ITC measurements, and Drs. R. Menard and J. D. Schrag for helpful comments.

■ ABBREVIATIONS

RAF, Ras-activated factor; MEK, MAPK/ERK kinase; ERK, extracellular signal-regulated kinase; EGF, epidermal growth factor; MP1, MEK partner 1; KSR, kinase suppressor of Ras; TEV, tobacco etch virus protease; IMAC, immobilized metal affinity chromatography; PBS, phosphate-buffered saline; SEC, size exclusion chromatography; CD, circular dichroism spectroscopy; ITC, isothermal titration calorimetry.

■ REFERENCES

(1) Skarpen, E., Flinder, L. I., Rosseland, C. M., Orstavik, S., Wierod, L., Oksvold, M. P., Skalhegg, B. S., and Huitfeldt, H. S. (2008)MEK1 and MEK2 regulate distinct functions by sorting ERK2 to different intracellular compartments. *FASEB J. 22*, 466–476.

(2) Severin, S., Ghevaert, C., and Mazharian, A. (2010)The mitogen-activated protein kinase signaling pathways: role in megakaryocyte differentiation. *J. Thromb. Haemost. 8*, 17–26.

(3) Mebratu, Y., and Tesfaigzi, Y. (2009)How ERK1/2 activation controls cell proliferation and cell death: Is subcellular localization the answer?. *Cell Cycle 8*, 1168–1175.

(4) Montagut, C., and Settleman, J. (2009)Targeting the RAF-MEK-ERK pathway in cancer therapy. *Cancer Lett. 283*, 125–134.

(5) Aoki, Y., Niihori, T., Narumi, Y., Kure, S., and Matsubara, Y. (2008)The RAS/MAPK syndromes: novel roles of the RAS pathway in human genetic disorders. *Hum. Mutat. 29*, 992–1006.

(6) Dard, N., and Peter, M. (2006)Scaffold proteins in MAP kinase signaling: more than simple passive activating platforms. *Bioessays. 28*, 146–156.

(7) McKay, M. M., and Morrison, D. K. (2007)Integrating signals from RTKs to ERK//MAPK. *Oncogene 26*, 3113–3121.

(8) Schaeffer, H. J., Catling, A. D., Eblen, S. T., Collier, L. S., Krauss, A., and Weber, M. J. (1998)MP1: a MEK binding partner that enhances enzymatic activation of the MAP kinase cascade. *Science 281*, 1668–1671.

(9) Michaud, N. R., Therrien, M., Cacace, A., Edsall, L. C., Spiegel, S., Rubin, G. M., and Morrison, D. K. (1997)KSR stimulates Raf-1 activity in a kinase-independent manner. *Proc. Natl. Acad. Sci U.S.A. 94*, 12792–12796.

(10) Kolch, W. (2005)Coordinating ERK/MAPK signalling through scaffolds and inhibitors. *Nat. Rev. Mol. Cell Biol. 6*, 827–837.

(11) Wunderlich, W., Fialka, I., Teis, D., Alpi, A., Pfeifer, A., Parton, R. G., Lottspeich, F., and Huber, L. A. (2001)A novel 14-kilodalton protein interacts with the mitogen-activated protein kinase scaffold mp1 on a late endosomal/lysosomal compartment. *J. Cell Biol. 152*, 765–776.

(12) Teis, D., Wunderlich, W., and Huber, L. A. (2002)Localization of the MP1-MAPK scaffold complex to endosomes is mediated by p14 and required for signal transduction. *Dev. Cell 3*, 803–814.

(13) Kurzbauer, R., Teis, D., de Araujo, M. E., Maurer-Stroh, S., Eisenhaber, F., Bourenkov, G. P., Bartunik, H. D., Hekman, M., Rapp, U. R., Huber, L. A., and Clausen, T. (2004)Crystal structure of the p14/MP1 scaffolding complex: how a twin couple attaches mitogen-activated protein kinase signaling to late endosomes. *Proc. Natl. Acad. Sci. U.S.A. 101*, 10984–10989.

(14) Lunin, V. V., Munger, C., Wagner, J., Ye, Z., Cygler, M., and Sacher, M. (2004)The structure of the MAP kinase scaffold MP1 bound to its partner p14: a complex with a critical role in endosomal MAP kinase signaling. *J. Biol. Chem. 279*, 23422–23430.

(15) Nada, S., Hondo, A., Kasai, A., Koike, M., Saito, K., Uchiyama, Y., and Okada, M. (2009)The novel lipid raft adaptor p18 controls endosome dynamics by anchoring the MEK-ERK pathway to late endosomes. *EMBO J. 28*, 477–489.

(16) Martin, B. R., and Cravatt, B. F. (2009)Large-scale profiling of protein palmitoylation in mammalian cells. *Nature Methods 6*, 135–138.

(17) Teis, D., Taub, N., Kurzbauer, R., Hilber, D., de Araujo, M. E., Erlacher, M., Offterdinger, M., Villunger, A., Geley, S., Bohn, G., Klein, C., Hess, M. W., and Huber, L. A. (2006)p14-MP1-MEK1 signaling regulates endosomal traffic and cellular proliferation during tissue homeostasis. *J. Cell Biol. 175*, 861–868.

(18) Guillaumot, P., Luquain, C., Malek, M., Huber, A. L., Brugiere, S., Garin, J., Grunwald, D., Regnier, D., Petrilli, V., Lefai, E., and Manie, S. N. (2010)Pdro, a protein associated with late endosomes and lysosomes and implicated in cellular cholesterol homeostasis. *PLoS ONE 5*, e10977.

(19) Hoshino, D., Tomari, T., Nagano, M., Koshikawa, N., and Seiki, M. (2009)A novel protein associated with membrane-type 1 matrix metalloproteinase binds p27(kip1) and regulates RhoA activation, actin remodeling, and matrigel invasion. *J. Biol. Chem. 284*, 27315–27326.

(20) Sancak, Y., Bar-Peled, L., Zoncu, R., Markhard, A. L., Nada, S., and Sabatini, D. M. (2010)Ragulator-Rag complex targets mTORC1 to the lysosomal surface and is necessary for its activation by amino acids. *Cell 141*, 290–303.

(21) Bryson, K., McGuffin, L. J., Marsden, R. L., Ward, J. J., Sodhi, J. S., and Jones, D. T. (2005)Protein structure prediction servers at University College London. *Nucleic Acids Res. 33*, W36–W38.

(22) Apweiler, R., Attwood, T. K., Bairoch, A., Bateman, A., Birney, E., Biswas, M., Bucher, P., Cerutti, L., Corpet, F., Croning, M. D., Durbin, R., Falquet, L., Fleischmann, W., Gouzy, J., Hermjakob, H., Hulo, N., Jonassen, I., Kahn, D., Kanapin, A., Karavidopoulou, Y., Lopez, R., Marx, B., Mulder, N. J., Oinn, T. M., Pagni, M., Servant, F., Sigrist, C. J., and Zdobnov, E. M. (2001)The InterPro database, an integrated documentation resource for protein families, domains and functional sites. *Nucleic Acids Res. 29*, 37–40.

(23) Vincentelli, R., Canaan, S., Campanacci, V., Valencia, C., Maurin, D., Frassinetti, F., Scappucini-Calvo, L., Bourne, Y., Cambillau, C.,

and Bignon, C. (2004)High-throughput automated refolding screening of inclusion bodies. *Protein Sci. 13*, 2782–2792.

(24) Chiu, J., March, P. E., Lee, R., and Tillett, D. (2004)Site-directed, Ligase-Independent Mutagenesis (SLIM): a single-tube methodology approaching 100% efficiency in 4 h. *Nucleic Acids Res. 32*, e174.

(25) Magnusdottir, A., Johansson, I., Dahlgren, L. G., Nordlund, P., and Berglund, H. (2009)Enabling IMAC purification of low abundance recombinant proteins from E. coli lysates. *Nature Methods 6*, 477–478.

(26) Uversky, V. N. (2002)Natively unfolded proteins: a point where biology waits for physics. *Protein Sci. 11*, 739–756.

(27) Groemping, Y., and Hellmann, N. (2005) (Coligan, J. E., Dunn, B. M., Speicher, D. W., and Wingfield, P. T., Eds.) John Wiley & Sons, Inc., Hoboken, NJ.

(28) Russo, A. A., Jeffrey, P. D., Patten, A. K., Massague, J., and Pavletich, N. P. (1996)Crystal structure of the p27Kip1 cyclin-dependent-kinase inhibitor bound to the cyclin A-Cdk2 complex. *Nature 382*, 325–331.

(29) Lacy, E. R., Filippov, I., Lewis, W. S., Otieno, S., Xiao, L., Weiss, S., Hengst, L., and Kriwacki, R. W. (2004)p27 binds cyclin-CDK complexes through a sequential mechanism involving binding-induced protein folding. *Nat. Struct. Mol. Biol. 11*, 358–364.